

ESTIMATION OF OBLIQUE, CONVEX AND CONCAVE SURFACE EFFECTS ON MICROACOUSTICALLY DETERMINED ELASTIC PARAMETERS

A. Doghmane and Z. Hadjoub

Laboratoire des Semi-Conducteurs, Département de Physique, Université de Annaba, Algeria.
a_doghmane@yahoo.fr

Abstract

Using the acoustic ray model for planar surfaces applied to acoustic microscopy investigations, we estimate the influence surface specimen inclination, α , as well as the influence of the specimen curvature radius of convex, or concave, surfaces, on the elastic parameters. It is found that Young's and shear moduli vary with surface tilting with a shift of up to 20% for a 35° inclination. A universal formula: $\Delta G/G = \Delta E/E = 1 - \cos\alpha$ is derived and used to determine the exact values of these constants. Similarly, for curved surfaces, it is shown that the curvature has a great effect on the determined elastic properties. Such effects are better investigated in terms $\Delta G/G$ and $\Delta E/E$, found to reach 20 % for small convex radii and even higher for concave surfaces.

Introduction

The scanning acoustic microscope [1, 2], SAM is becoming one of the most promising and challenging tools for nondestructive, non contaminating and non contacting investigations. It is receiving a great deal of interest by, materials scientists, biologists, researchers in the field of applied mechanics, physics and mathematics due to its potential applications in the study of materials in many fields: crystallography, biology, industry, microelectronics, micro-metallurgy. Such an instrument can be used to measure propagating wave velocities in order to determine elastic constants, anisotropy, thin film characteristics, anisotropy, to study of living cells.

One major advantage of the SAM method is its application to samples without any prior preparations. Hence, planar, inclined, convex and concave specimen could be investigated. However, mathematical and physical models proposed to explain experimental results [3, 4] have to be modified according to the geometry of the specimen which greatly affects the reflected acoustic beam paths causing variable phase differences between generated and reflected beams ; leading thus to different acoustic materials signatures and hence variable wave velocities of the propagating modes. To overcome such difficulties and to be able to introduce necessary corrections in order to obtain real parameter values we propose the application of the acoustic ray model to tilted surfaces [5, 6] and

nonplanar (convex and concave) surfaces [7, 8]. Only few typical results are presented.

Scanning acoustic microscopy principle

Figure 1a shows a schematic diagram of a SAM working in the reflection mode. The acoustic signal generated by a piezoelectric transducer propagates into a delay line (usually a sapphire rod) at the end of which a spherical lens is manufactured. Such a lens focuses the acoustic beam either on the surface or into the subsurface of the sample through a coupling liquid that ensures good wave propagation. After having scanned the specimen, the reflected beam (full of information) will be collected by the transducer that acts now as a receiver

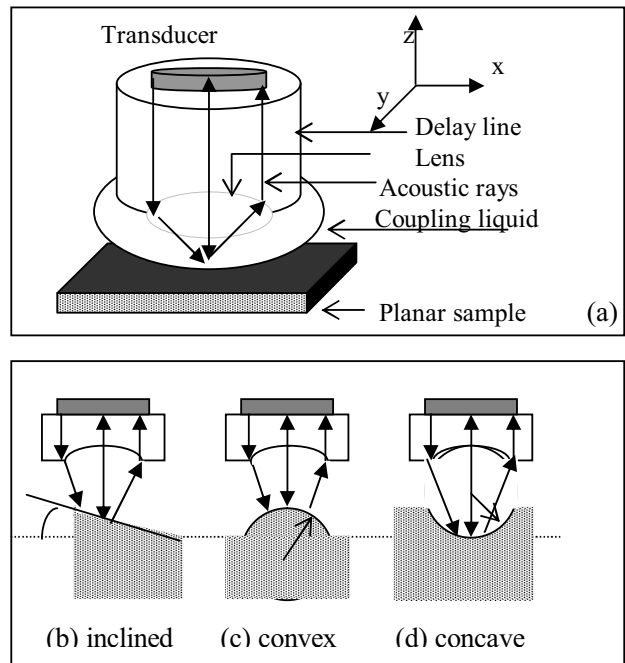


Figure 1: Schematic diagram of the acoustic part of a SAM, in the reflection mode, applied to planar, inclined, convex and concave surfaces.

The principle of quantitative micro-characterization (or microanalysis) is based on the measurements of the so-called acoustic materials signatures, also known as $V(z)$. These signatures are obtained by recording the output signal, V , as a function of defocusing distance, z , when the sample is displaced along the z axis between the focal plane and the lens. Such a response is the result of constructive

and destructive interference between many leaky waves [9] whose determined velocities give valuable information on elastic properties.

Acoustic Ray Model

Planar surfaces

The acoustic ray model for planar surfaces was first proposed by Parmon and Bertoni [3]. According to this model, simple calculations of the phase difference, $\Delta\phi$, between axial mode and leaky Rayleigh wave phases give:

$$\Delta\phi = 4\pi fz(1 - \cos\theta_R)/V_R \sin\theta_R \quad (1)$$

where f is the operating frequency, z the distance from the focal plane, and θ_R the critical angle at which a Rayleigh wave leaks its energy back into the liquid when propagating along the liquid/solid interface with a characteristic velocity V_R . Periodical deep minima, with a constant spacing are found for $\Delta\phi = 2\pi$. The period, Δz , between two successive minima or two successive maxima in the $V(z)$ responses is then given by:

$$\Delta z = V_R \sin\theta_R / 2f(1 - \cos\theta_R) \quad (2)$$

Under usual operating SAM conditions, this period is related to Rayleigh velocity, V_R , of the most predominant propagating mode, by the relation:

$$V_R = V_{liq} / [1 - (1 - V_{liq}/2f\Delta z)^2]^{1/2} \quad (3)$$

Inclined surfaces

Most research work was concerned with planar objects onto which different types of SAWs propagate with typical characteristic velocities, but little was devoted to inclined or nonplanar surfaces. For inclined surfaces, following the same steps as those proposed for planar objects and taking into account the sample inclination of α degree (Fig. 1b), the apparent phase difference between the axial and Rayleigh rays is found to be, after all calculations and simplifications

$$\Delta\phi_a = \Delta\phi / \cos\alpha \quad (4)$$

Therefore, the period of flat surfaces, Δz , would be different from apparent periods, Δz_a , for oblique surfaces. Hence, one can readily write:

$$\Delta z_a = \Delta z \cos\alpha \quad (5)$$

It is clear that both $\Delta\phi_a$ and Δz_a are function of not only the specimen characteristics but the inclination angle as well. More over we notice that for a null inclination ($\alpha = 0$) we obtain the expressions 1 and 2 of planar surfaces. The expression of apparent Rayleigh velocity, V_{Ra} , for oblique objects, is obtained

when Δz is replaced by Δz_a in relation 3. Hence, the apparent Rayleigh velocity becomes [6]:

$$V_{Ra} = V_{liq} / \{1 - [1 - (1/\cos\alpha)(1 - \sqrt{1 - (V_{liq}/V_R)^2}]^2\}^{1/2} \quad (6)$$

Nonplanar surfaces

SAWs can exist on surfaces with simple or arbitrary curvature; in the latter case the situation becomes considerably more complex and much less well understood. Therefore, the acoustic ray model applied to SAM configuration can be modified to take into account the curvature radius effects, r_c . This is illustrated by figures 1c and 1d where it can be seen that the reflected wave reaches the transducer after having scanned the arch rather than the straight line normally taken in the planar case. Thus, following the same steps as for planar model and taking into account wave paths, the phase differences for convex, $\Delta\phi_{cv}$, or concave, $\Delta\phi_{cc}$, objects becomes [7]:

$$\frac{4\pi f}{V_{liq}} \left\{ \mp r_c \cos\theta_R \pm \sqrt{r_c^2 \cos^2\theta_R + z^2 \mp 2zr_c} + z + r_c \sin\theta_R \right. \\ \left. \arccos \left[1 \mp \frac{\mp z^2 + r_c \cos\theta_R - \sqrt{r_c \cos^2\theta_R + z^2 \mp 2zr_c}}{2r_c(r_c \mp z)} \right]^2 \right\} \quad (7)$$

where the upper and lower signs stand for convex and concave surfaces, respectively. This relation, when computed, allows the determination of apparent acoustic parameters (periods, velocities, elastic constants, etc.)

Inclined surfaces effects

The effects of inclination on apparent Rayleigh velocity is better described by relation (6): it decreases as α increases. This dependence, that coserves a similar trend, changes in magnitude for each material, as a result of the presence in the expression of V_R which is a characteristic of each solid. Therefore, to overcome such a limitation, we investigated relative variations, i.e. we normalize the shift of each material to its own characteristic Rayleigh velocity. Simple calculations of $\Delta V/V$ give:

$$\Delta V/V = |V_{Ra} - V_R| / V_R = 1 - \sqrt{\cos\alpha} \quad (8)$$

This formula shows the inclination effects on apparent velocity. Its universality comes from the fact that it can be applied to all types of materials. This behavior is better illustrated in figure 2a displayed in terms of relative velocity variations as a function of α . It is clear that for small inclination angles one obtains errors of few percents only, whereas for higher sample tiltings errors of 10% can be introduced

Since elastic constants (Young's modulus, E and shear modulud, G) depend on proapagating wave velocities they should be influenced by surface inclinations. Using familiar relations of elastic

constants and following the same procedure as above, we derive expressions of relative variations of elastic constants such that $\Delta E/E = |E - E_a|/E$ and $\Delta G/G = |G - G_a|/G$ to find after all calculations and simplifications the following relation:

$$\Delta E/E = \Delta G/G = 1 - \cos\alpha \tag{9}$$

A close analysis of this expression shows relative that variations of both Young's modulus and shear modulus have the same behavior in trend and in magnitude. This universal dependence (for all materials and both elastic constants) is better illustrated in figure 2b. It can be seen that as the inclination angle increases the introduced errors increase as well to approach values as high as 20 % for $\alpha \approx 35^\circ$. The importance of such curves (Fig. 2) lies not only in the correction of measured acoustic parameters when the inclination is known and vice versa but in their universal applicability for all types of materials: heavy, light, medium, slow, fast, etc.

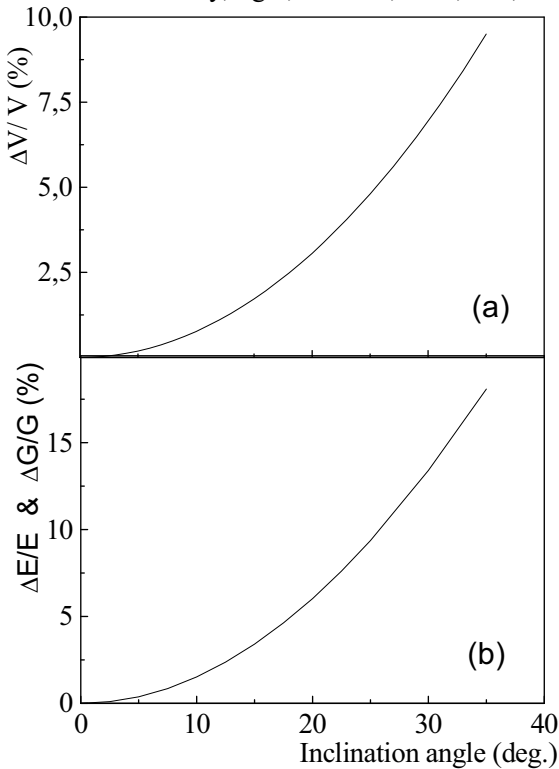


Figure 2 Inclination effects on relative variations of (a) Rayleigh velocity and (b) elastic constants.

Nonplanar surfaces effects

Defocusing effects on apparent periods

The quantified effects of curvature radii on experimental acoustic materials signatures were first reported by Hadjoub *et. al.* [7]. In the present paper, we make use of the relation (7) to calculate apparent periods Δz_c as a function of defocusing distances, z .

this is accomplished, when $\Delta\phi_a = 2\pi$, for a series of calculations carried out on several planar structures. Typical specimen defocus dependence on apparent periods is better illustrated in figure 3, for which a radius of 2.75 mm was chosen for both convex and concave materials: quartz ($\square \square \square \square$), glass ($\diamond \diamond \diamond \diamond$), stainless-steel ($\Delta \Delta \Delta \Delta$) and tungsten ($\circ \circ \circ \circ$). The upper set of curves was obtained for concave structures, whereas the lower set for convex materials. It is clear that, for increasing defocusing distances z , apparent periods Δz_c of each material decrease for convex structures and increase for concave surfaces. The onset of Δz_c variation near the focal point ($z = 0$), represents the Δz periods of the given material having a planar surface. This onset differs from one material to the other as a result of their distinct acoustic parameters.

For small values of z , near the focal point, no much change would be expected because the distance traveled by Rayleigh waves on the arc is so small that it can be considered as a straight line. Therefore, apparent periods remain almost constant for both concave and convex structures and approaches the values of planar surfaces of a given material.

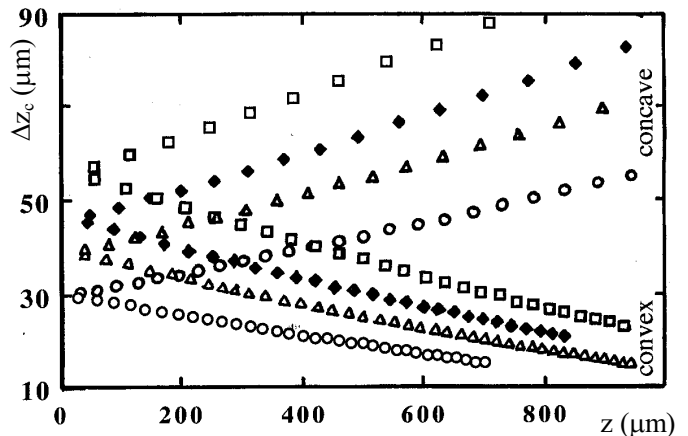


Figure 3 Defocusing distance effects on apparent periods for convex and concave quartz ($\square \square \square \square$), glass ($\diamond \diamond \diamond \diamond$), stainless-steel ($\Delta \Delta \Delta \Delta$) and W ($\circ \circ \circ \circ$).

Curvature radii effects on apparent periods

To investigate the effects of curvature radii on apparent periods, we repeated the above analysis for each convex and concave material but with varying diameters. The resulting behaviors of the curves were so similar that any comments which apply to glass will also apply to tungsten, stainless steel and quartz. Figure 4 illustrates typical variations of calculated apparent periods Δz_c for concave and convex structures, as a function of curvature radii r_c at a defocusing distance $z = 500 \mu\text{m}$. It is clear that the general trend of these curves, when r_c increases, is: an

increase of Δz_c for convex materials but a decrease for concave structures

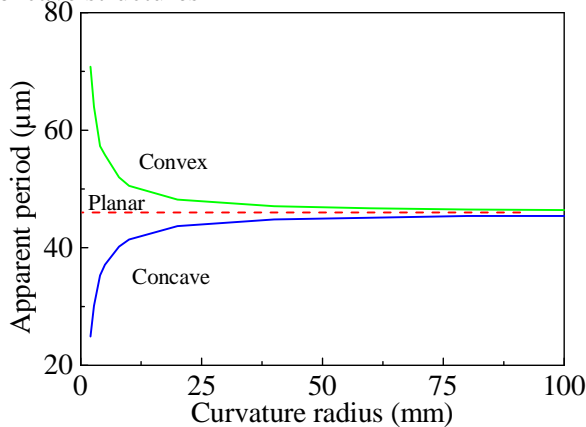


Figure 4 Calculated apparent periods Δz_c , for convex and concave glass structures versus curvature radii, together with the periods of its planar surfaces (- - -)

Curvature radii effects on elastic constants

The influence of curvature radii on elastic constants is a consequence of their dependence on velocities; the latter parameters depend in turn on periods. Such effects are better illustrated in figure 5 in terms of relative elastic constants, $\Delta E/E$ and $\Delta G/G$ as function of curvature radii for convex (a) and concave (b) glass materials.

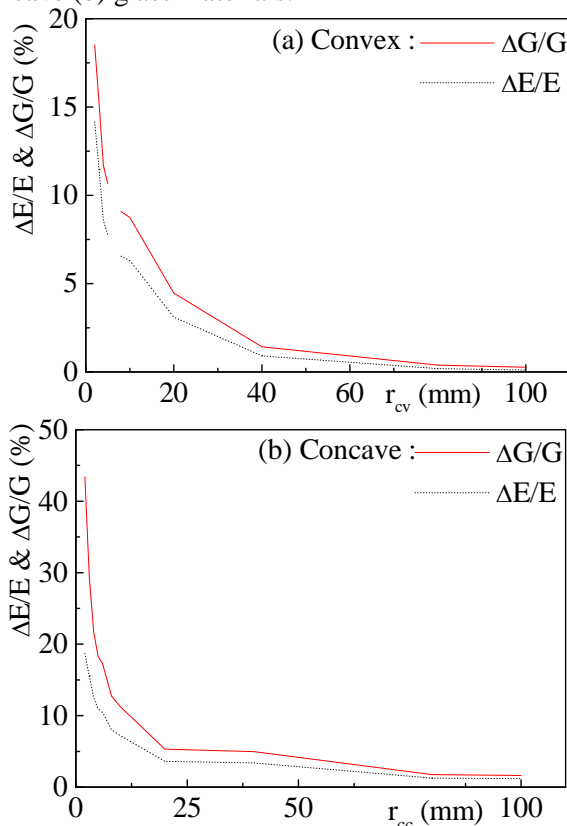


Figure 5 Relative variations of elastic constants for convex (a) and concave (b) glass materials.

It is clear that for shift, from real values of up to 20% were obtained for small convex radii; these shifts for concave structures are even higher. Whereas, as the radii increase the curves decrease; this is due to the fact that the surface arch gets wider until it tends towards a straight line. Therefore, the curves tend asymptotically to zero, i.e. towards the planar surface real values. Such curves are important in introducing correction to measure, via a SAM, exact elastic parameters of convex or concave surfaces or find the concavity and convexity radii.

Conclusion

The influence of inclination angles, convexity and concavity of different materials on elastic parameters is put into evidence via the application and/or the modification of the acoustic ray model. Hence, it is shown that the effect of the geometry of the samples can be corrected to get their real measured values, when a SAM is used, without any prior surface geometric preparation

References

- [1] P. V. Zinin “ Quantitative acoustic microscopy” in Handbook of Elastic Properties of Solids, Liquids and Gases vol. 1.”, edited by: Levy, Bass and Stern (Acad. Press, N.Y.) 2001, pp 187-226,
- [2] Andrew Briggs, (ed.), Advances in Acoustic microscopy, Plenum Press, New York, 1995.
- [3] W. Parmon and H. L. Bertoni, “Ray interpretation the material signature in the acoustic microscope” Elect. Lett. vol. 15, pp 684-686, 1979
- [4] C. G. R. Sheppard and T. Wilson, “Effects of Hugh Angle of convergence of $V(z)$ in the scanning acoustic microscopy” Appl. Phys. Lett. vol. 38, pp. 858-859, 1981.
- [5] R.D. Weglein, “Acoustic microscopy of curved surfaces” Appl. Phys. Lett. vol. 38, pp 516-518, 1981
- [6] Z. Hadjoub. A. Doghmane and A. Hamel “Influence of inclined surfaces on Rayleigh velocities in acoustic microscopy” Elect. Lett. vol. 27, pp 537-539, 1991.
- [7] Z. Hadjoub, A. Doghmane R. Caplain, J. M. Saurel and J. Attal , “Acoustic microscopy investigations of nonplanar surfaces ” Elect. Lett. vol. 33, pp 105-107, 1997.
- [8] K. I. Maslov, P.V.Zinin, O. I. Lobkis and T. Kundu, “ $V(z)$ curve formation of solid spherical micoparticles in scanning acoustic microscopy” J. Microsc. vol. 178, pp 125-133, 1995
- [9] J. Kushibiki and N. Chubachi, “Material characterization by line-focus-beam scanning acoustic microscopy” IEEE Trans.UltrasonJ. Microsc. vol. 32, pp 189-212, 1985.